A Color LED Driver Implemented by the Active Clamp Forward Converter

C. H. Chang, H. L. Cheng, C. A. Cheng, E. C. Chang*

Power Electronics Laboratory, Department of Electrical Engineering
I-Shou University, Kaohsiung City 84001, Taiwan
*enchihchang@isu.edu.tw

ABSTRACT
Because light emitting diodes (LEDs) have the advantages of dc working voltage, high luminescent efficiency, short ignition time, high reliability and pollution free, they have substituted for incandescent bulbs and fluorescent lamps gradually. In order to simplify circuit complexity, an active clamp forward converter with the sequential color display (SCD) control is proposed to drive red, green and blue (RGB) LED arrays. The proposed converter has zero-voltage switching (ZVS) operations of both the main switch and the auxiliary switch, resulting in high system efficiency. Driving RGB LED arrays sequentially by one converter can save components and reduce cost significantly. Additionally, the pulse-width modulation (PWM) control is applied to achieve a large chromaticity variation. The circuit operations are analyzed in detail and the circuit parameters are designed based on the practical considerations. Finally, an illustrative example is implemented to demonstrate the feasibility and validity of the proposed LED driver.

Keywords: Light emitting diode (LED), active clamp forward converter, sequential color display (SCD).

1. Introduction

Recently, light emitting diodes (LEDs) have substituted for incandescent bulbs and fluorescent lamps gradually in the residential, industrial and commercial lighting applications [1], because they have the advantages of dc working voltage, high luminescent efficiency, short ignition time, high reliability and pollution free, etc. Moreover, since mixing multi-coloured LEDs can provide a large chromaticity variation, LEDs are progressively used in outdoor landscape lighting systems as well.

Figure 1 shows the block diagram of a photovoltaic powered landscape lighting system, in which an isolated DC/DC converter is used to fulfill a step-down conversion, govern the current through LED arrays and provide the electrical isolation of safety requirements. Generally, a colored LED module is composed of red, green and blue (RGB) LED arrays. Since RGB LEDs have different electrical characteristics, three isolated DC/DC converters are required to regulate the current through each LED arrays [2]. Therefore, the number of power components will become triple, resulting in large volume, high cost and low reliability.

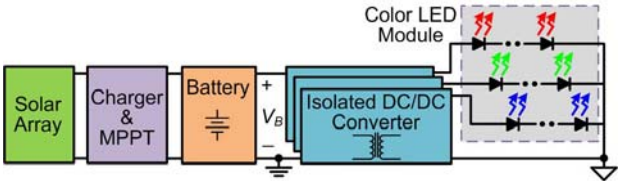

Figure 1. The block diagram of a photovoltaic powered landscape lighting system.

In the literature [3, 4], a sequential color scanning scheme was proposed to reduce power consumption. LEDs are very suitable for a sequential color display (SCD) due to their fast response. When LEDs are displayed intermittently with high frequency, human cannot observe the darkness of short time intervals. The SCD control has been applied in a color LED backlight driving system for liquid crystal display (LCD) panels [5], [6], in which RGB LED arrays are sequentially driven by the same DC/DC converter.

Many isolated DC/DC converters for RGB LED driving, such as flyback and forward converters, have been presented in the literature [3, 5].

However, their hard-switching operations reduce conversion efficiency and induce electromagnetic interference (EMI) noise. This paper proposes an active clamp forward converter [7 – 9] with SCD control as the color LED driver for a photovoltaic powered landscape lighting system. For this driver, due to saving transformers, power switches, control ICs and energy storage components, the circuit complexity can be simplified, and the system volume and cost can be significantly reduced. With accurate analysis and design, both of the main switch and the auxiliary switch can turn on under zero-voltage switching (ZVS), leading to higher system efficiency and lower EMI noise. Besides, the pulse-width modulation (PWM) control is applied to change the luminance of RGB LEDs so that a large chromaticity variation can be achieved. The operation principles are addressed. Experimental results of a 100 W laboratory prototype are used to verify the feasibility and validity of the theoretical predictions.

2. Operation principles

The proposed color LED driver, as shown in figure 2, consists of an active clamp forward converter and RGB LED arrays with SCD control. In this section, the operation principles of the SCD control and the proposed converter are introduced briefly in the following.

2.1 Sequential color display control

To achieve SCD control, RGB LED arrays are connected in series with the switches S_R, S_G and S_B, respectively. The switches are driven with phase-shift manner, as illustrated in figure 3, in which v_{GS_R}, v_{GS_G} and v_{GS_B} are their gate signals with the switching frequency f_m. The frequency of the driving signals v_{GS1} and v_{GS2} in the active clamp forward converter is f_s which should be much higher than f_m. The voltages V_{o_R}, V_{o_G} and V_{o_B} are the forward voltage of RGB LED arrays, respectively. The currents i_R, i_G and i_B are their corresponding driving currents.

Assuming that the currents i_R, i_G and i_B have the same amplitude I_P at full-load condition, the maximum average output-current $I_{o,avg}$ of a conventional RGB LED driver is $3I_P$. For the proposed driver, if the maximum duty cycle of the driving signals v_{GS_R}, v_{GS_G} and v_{GS_B} are D_{max}, then the maximum average output-current $I_{o,avg}$ is

$$I_{o,avg} = I_P \times D_{max} \times 3 \tag{1}$$

Because D_{max} is 33.33% in the proposed driver, $I_{o,avg}$ is only equal to I_P. Therefore, the required output-power of the proposed driver is only one-third of that of a conventional driver, which results in energy saving significantly.

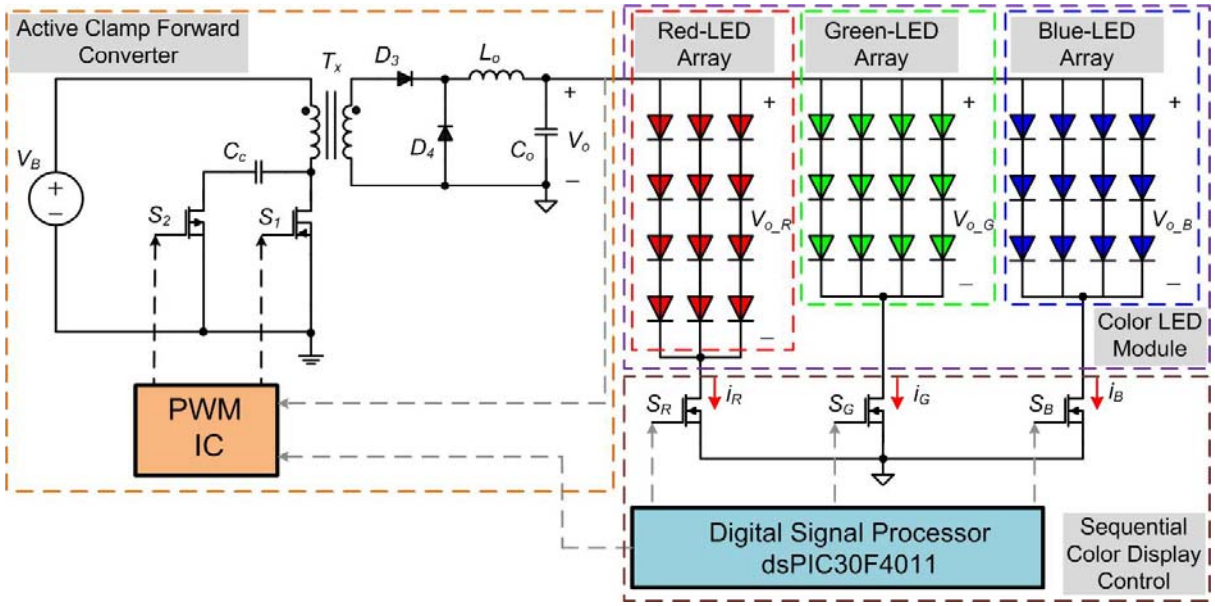

Figure 2. The conceptual circuit of the proposed color LED driver with SCD control.

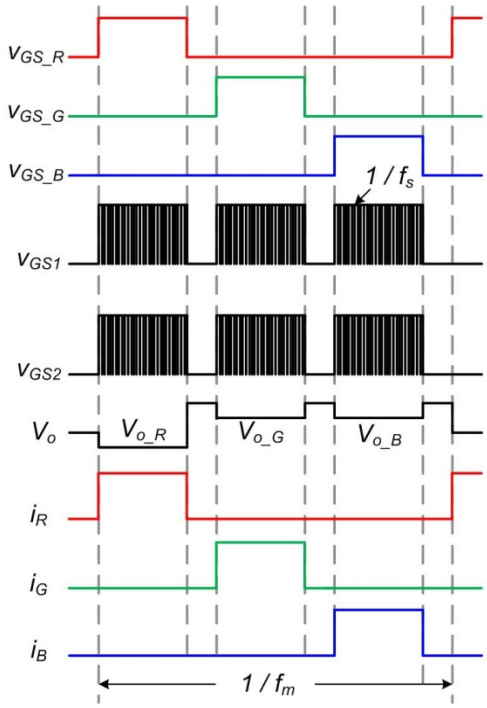

Figure 3. Driving signals and conceptual key waveforms of the SCD control.

In the proposed system, the red, green and blue LED arrays are driven by the same converter sequentially, leading to small volume, low cost and high reliability. All of the driving signals v_{GS_R}, v_{GS_G} and v_{GS_B} are produced by the digital signal processor (dsPIC30F4011). The luminance of each LED array is dimmable by modulating the duty of its driving signal, so as the color of the RGB-LED module is variable. The output capacitor C_o with low capacitance is used in the converter so that the output voltage can vary promptly according to the forward voltage of each LED array.

2.2 Active clamp forward converter

Figure 4 shows the circuit diagram of the active clamp forward converter. Each active switch S_1 (S_2) is composed of an MOSFET Q_1 (Q_2) and its intrinsic anti-parallel diode D_1 (D_2). The forward converter is formed by the main switch S_1, transformer T_x, forward diode D_3, freewheel diode D_4, output inductor L_o, and output capacitor C_o. Instead of the reset winding in traditional forward converter, the auxiliary switch S_2 and the clamping capacitor C_c are used to reset the residual flux of transformer. The residual energy of magnetizing inductor L_m can be restored to the input voltage source. Both of the main switch S_1 and the auxiliary switch S_2 can turn on under ZVS, resulting in low switching losses and high system efficiency.

For simplifying the analysis of operation principles, following conditions are made:

1) All components are ideal.

2) The capacitance of C_c is much higher than that of the intrinsic capacitor C_{ds}, and the inductance of L_m is much higher than that of the leakage inductor L_r.

3) L_o and C_o are large enough so that the output voltage V_o and output current I_o can be regarded as constant.

4) The dead time between the driving signals of S_1 and S_2 is very short and negligible. The turn-on intervals of S_1 and S_2 are considering as DT_s and $(1\text{-}D)T_s$, in which T_s is the switching period in steady-state operation.

According to the volt-second balance concept, the relation of input voltage V_B and the voltage across clamping capacitor v_c can be expressed as

$$V_B DT_s = (v_c - V_B)(1-D)T_s \tag{2}$$

Arranging Eq. 2 yields

$$v_c = \frac{1}{(1-D)} V_B \tag{3}$$

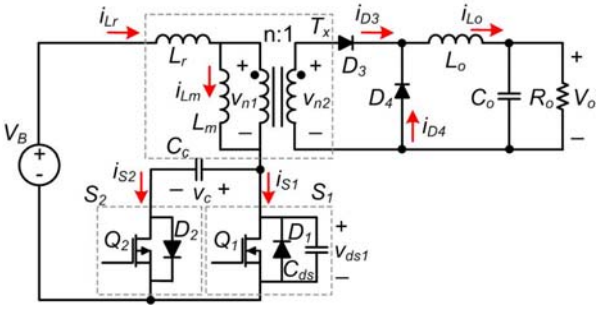

Figure 4. Circuit diagram of the active clamp forward converter.

Eq. 3 indicates that v_c is the output of boost-type operation with input voltage V_B. When S_1 turns off and S_2 turns on, the voltage across main switch v_{ds1} will be equal to v_c and determined as

$$v_{ds1} = v_c = \frac{1}{(1-D)} V_B \quad (4)$$

Figure 5 shows the theoretical waveforms of the active clamp forward converter, which is divided into nine operation modes within one switching period. The operation principle of each mode will be introduced referring to the equivalent circuits shown in figure 6.

Mode 1 (t_0 ~ t_1): At the moment t = t_0, the switch S_1 is turning on, and the switch S_2 is turning off. Since the voltage across magnetizing inductor v_{n1} is equal to V_B, its current i_{Lm} increases linearly. The voltage across secondary winding v_{n2} is V_B / n so that the forward diode D_3 turns on and the freewheel diode D_4 turns off. The input voltage source charges output inductor L_o through the transformer T_x and D_3. This mode ends while the gate signal of S_1 disappears.

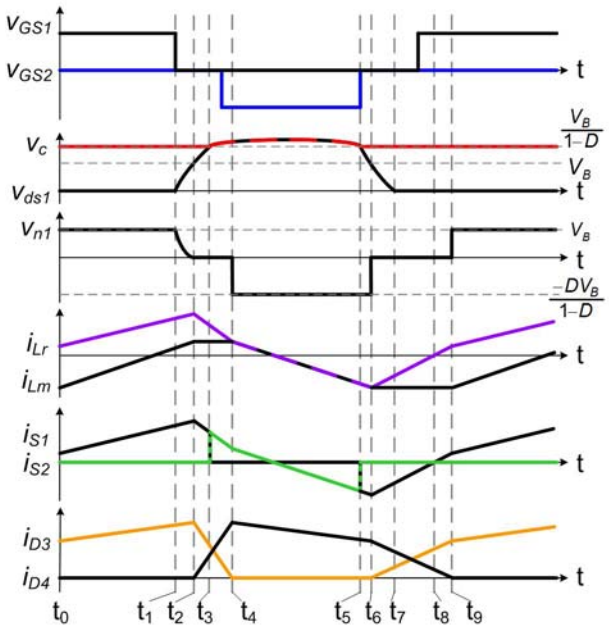

Figure 5. Theoretical waveforms of the active clamp forward converter.

Mode 2 (t_1 ~ t_2): At the moment t = t_1, the main switch S_1 turns off, and the current i_{Lr} charges the intrinsic capacitor C_{ds} of main switch. The voltage v_{ds1} increases, and the voltage v_{n1} decreases. This mode ends while v_{ds1} reaches V_B.

Mode 3 (t_2 ~ t_3): At the moment t = t_2, the voltage v_{n1} reaches zero so that D_3 and D_4 are both turn-on. Since the diode current i_{D3} decreases, the leakage inductor current i_{Lr} decreases as well. The magnetizing inductor current i_{Lm} remains the same. This mode ends while v_{ds1} reaches V_B / (1-D).

Mode 4 (t_3 ~ t_4): At the moment t = t_3, the main switch S_1 turns off. The current i_{Lr} flows through anti-paralleled diode D_2 to transfer energy to the clamping capacitor C_c, which provides ZVS operation for the auxiliary switch S_2 turn-on. Gate signal of S_2 should be applied during this mode. This mode ends while i_{D3} reaches zero.

Mode 5 (t_4 ~ t_5): At the moment t = t_4, because the current i_{D3} is zero, the inductor L_m is in series with L_r and participates in the resonance with C_c. The voltage v_{n1} is DV_B / (1-D) with reverse polarity. The resonant current i_{Lr} is equal to the current i_{Lm} and remains decreasing. While i_{Lr} becomes negative during this mode, the energy of L_m will be restored to the input voltage source. This mode ends while the gate signal of S_2 disappears.

Mode 6 (t_5 ~ t_6): At the moment t = t_5, the auxiliary switch S_2 turns off, and the resonant current i_{Lr} follows through the intrinsic capacitor C_{ds} to discharge it. This mode ends while the voltage v_{ds1} decreases to V_B.

Mode 7 (t_6 ~ t_7): At the moment t = t_6, the voltage v_{ds1} is equal to V_B so that the voltage v_{n1} becomes zero again. Since D_3 are turning on now, its current i_{D3} increases and the current i_{Lr} increases as well. The magnetizing inductor current i_{Lm} remains the same. This mode ends while v_{ds1} reaches zero.

Mode 8 (t_7 ~ t_8): At the moment t = t_7, the current i_{Lr} flows through anti-paralleled diode D_1 to transfer energy back to the input voltage source, which provides ZVS operation for the main switch S_1 turn-on. Gate signal of S_1 should be applied during this mode. The current i_{Lr} increases from negative with the slope of V_B / L_r. This mode ends while i_{Lr} reaches zero.

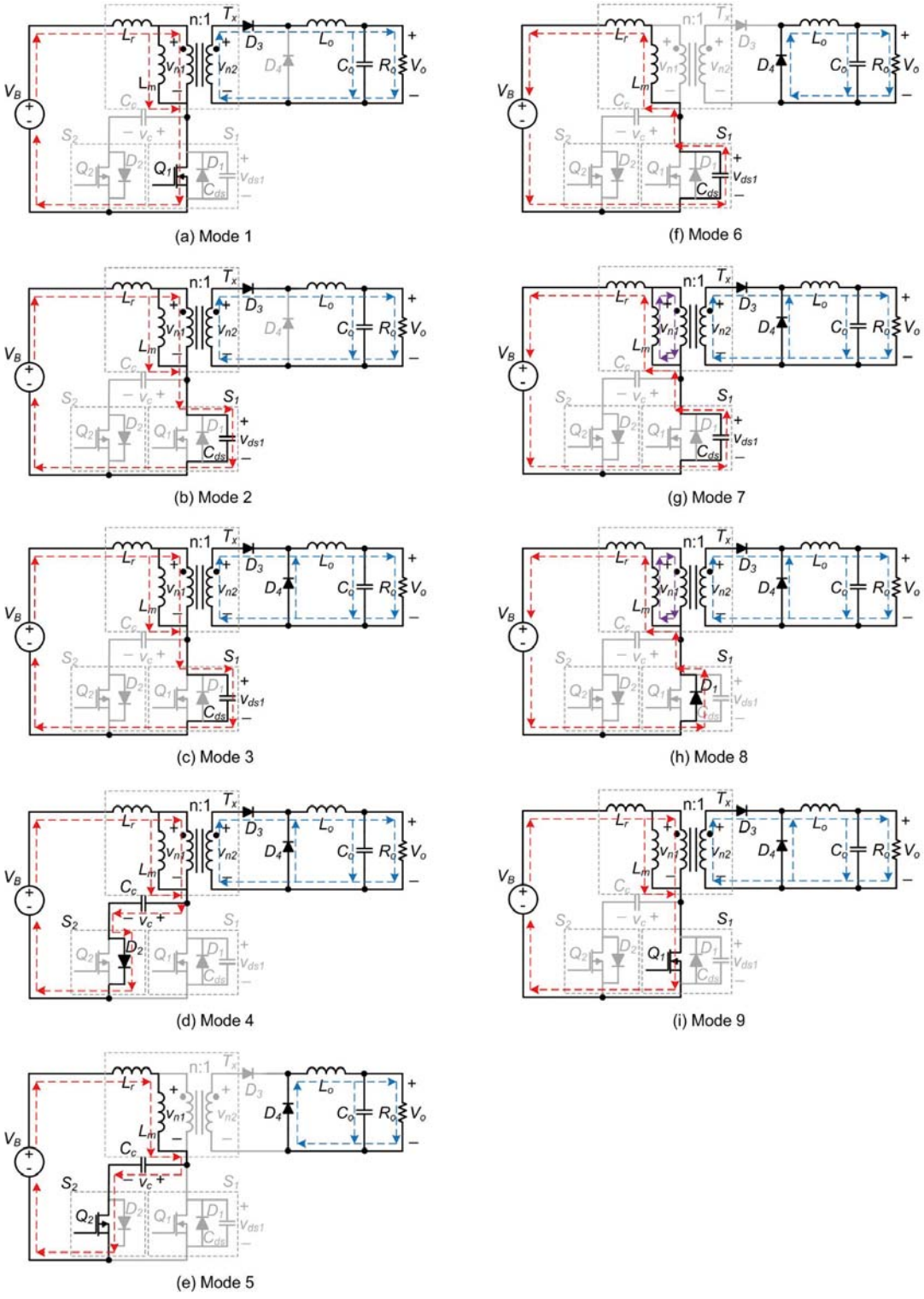

Figure 6. Equivalent circuits of operation modes.

Mode 9 ($t_8 \sim t_9$): At the moment $t = t_8$, the current i_{Lr} becomes positive. The current i_{D4} is decreasing continuously, and this mode ends when i_{D4} reaches zero. When the diode D_4 is turned off at $t = t_9$, the operation goes to Mode 1 of the next high-frequency switching cycle.

3. Design procedures

Based on the operation principles presented previously, the proposed color LED driver with the specifications listed in table 1 is taken as an illustrative example. The designed procedures of the active clamp forward converter are described as follows.

Step 1-Select f_s and D: Select the switching frequency f_s as 150 kHz. For the normal operation condition with 24 V battery voltage and full load output, the duty ratio D of the main switch S_1 is determined as 0.5.

Step 2-Determine n: Considering that the forward voltage V_f of the diode D_3 is around 0.7 V, the minimum turn ratio (n) of the transformer T_x can be determined as

$$n \geq \frac{V_B \cdot D}{(V_o + V_f)} \cong 0.99 \tag{5}$$

In the illustrative case, (n) is set as 1.

Step 3-Determine L_o: In order to minimize the output ripple current and reduce the current stress of power components, we select 10% of maximum output current as the boundary condition. The boundary inductance of L_o can be obtained as

$$L_{oB} = \frac{V_o \cdot (1-D)}{2 \cdot I_{oB} \cdot f_s} \cong 95\mu H \tag{6}$$

In the illustrative case, L_o is set at 100 μH.

Step 4-Determine C_o: While output inductance L_o is determined, considering that the specification of ΔV_o is 10 mV, the capacitance of C_o can be obtained

$$C_o = \frac{(1-D)}{8 L_o f_s^{\,2}} \cdot \left(\frac{V_o}{\Delta V_o} \right) = 31.7\mu F \tag{7}$$

input voltage, V_B	18 ~ 36 V_{dc}
output voltage, V_o	11.4 V_{dc}
maximum output current, I_o	2 A
ripple of output voltage, ΔV_o	10 mV_{pp}
switching frequency, f_s	150 kHz

Table 1. Electrical Specifications of the Prototype.

The standard capacitance with 33 μF is selected for C_o.

Step 5-Determine n_1: Select core material as TDK PC40 and core size as EE-19. Its saturation flux density B_{sat} is 4500 G at 60 °C, and effective cross area A_e is 0.23 cm^2. To avoid core saturation, we set the maximum flux density B_{max} at half of B_{sat}. Therefore, the turn number of primary winding n_1 can be calculated as

$$n_1 = \frac{V_B D T_s}{2 B_{max} A_e} = 7.7 \tag{8}$$

In the illustrative case, n_1 is set as 8. The inductance of L_m can be measured as 80 μH.

Step 6-Determine L_r: According to the operation principle of Mode 6, the current i_{Lr} at $t = t_6$ can be obtained from following

$$\left| i_{Lr}(t_6) \right| = \frac{D V_B}{2 L_m f_s} = 0.5A \tag{9}$$

To achieve ZVS operation of the main switch S_1, the inductance of L_r should meet following equation

$$L_r > \frac{C_{ds} V_B^{\,2}}{\left| i_{Lr}(t_6) \right|^2} \tag{10}$$

Considering that the intrinsic capacitor C_{ds} of IRF530 is 190 nF, the required inductance of L_r can be obtained as 438 nH.

Step 7-Determine C_c: To optimize the voltage stresses of C_c, S_1 and S_2, the period of the resonance occurring during S_1 turning-off should

be longer than ten times of the turn-off time of S_1, which is expressed as

$$2\pi\sqrt{(L_r + L_m)C_c} \geq 10 \times (1-D)/f_s \quad (11)$$

Thus, the minimum capacitance of C_c can be obtained as

$$C_c \geq \frac{100(1-D)^2}{(L_r + L_m)(2\pi f)^2} = 350nF \quad (12)$$

The standard capacitance with 470 nF is selected for C_c.

The calculated component parameters of the illustrative example are summarized in table 2.

4. Experimental results

While input voltage V_B is 24 V, figure 7 shows the measured waveforms of the output voltage V_o and the output inductor current i_{Lo} at full load operation. It can be seen that V_o is regulated at 11.41 V, and the average output current is 2.04 A, which are very close to the required specifications. The measured waveform of clamping capacitor voltage V_c according the driving signal V_{GS1} is shown in figure 8. It is obvious that resonance with the frequency determined by C_c and (L_r + L_m) occurs after the main switch S_1 is turning off. In this time interval, the resonant current i_{Lr} transfers energy from L_m to C_c, and then restores energy to the input voltage source.

main switch, S_1	IRF530 (100V/10A)
auxiliary switch, S_2	IRF9540 (100V/19A)
diodes, D_3, D_4	SB1060 (60V/10A)
leakage inductor, L_r	438 nH
magnetizing inductor, L_m	80 μH
clamping capacitor, C_c	0.47 μF
output inductor, L_o	100 μH
output capacitor, C_o	33 μF
transformer turn ratio, n:1	1:1

Table 2. Component Parameters of the Prototype.

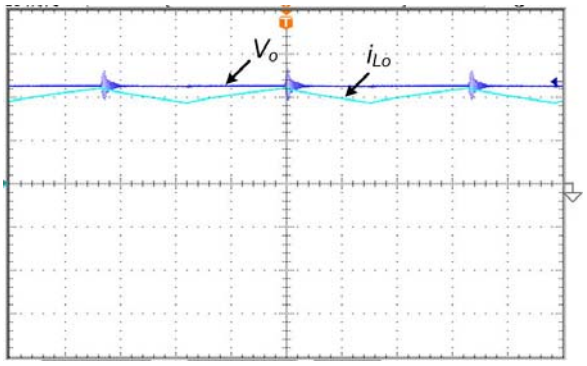

Figure 7. Measured waveforms of the output voltage V_o and the output inductor current i_{Lo} at full load operation (V_o: 5 V/div; i_{Lo}: 1 A/div; time: 2 μs/div).

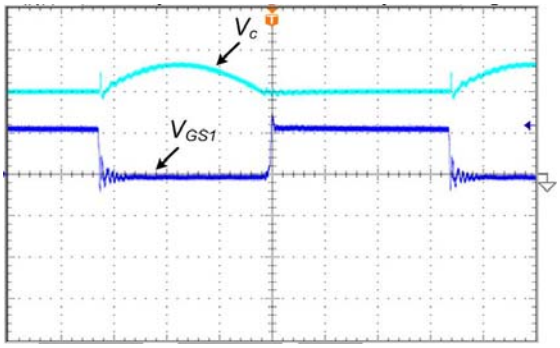

Figure 8. Measured waveforms of clamping capacitor voltage V_c according the driving signal V_{GS1} (V_{GS1}: 10 V/div; V_c: 20 V/div; time: 1 μs/div).

Figure 9 shows the measured voltage and current waveforms of the main switches S_1 at full load condition. It could be observed that S_1 can turn on under ZVS condition. Figure 10 shows the measured voltage waveforms of the auxiliary switches S_2 at full load condition. The drain to source voltage v_{ds2} becomes zero before the driving signal V_{GS2} is supplied, from which the ZVS operation of S_2 can be verified. Therefore, the switching losses can be significantly minimized to improve system efficiency.

Figure 11 shows the measured efficiency curve of the proposed color LED driver with 24 V input voltage. The maximum efficiency is up to 92.5% at I_o = 1.6 A. The normal operating range for driving color LED arrays is from 1.2 A to 1.8 A. The system efficiency can be kept above 91% in this range, which provide energy saving significantly.

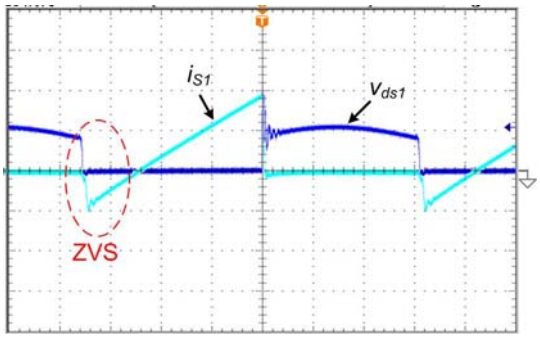

Figure 9. Measured voltage and current waveforms of the main switch S_1 at full load operation (v_{ds1}: 50 V/div; i_{S1}: 5 A/div; time: 1 μs/div).

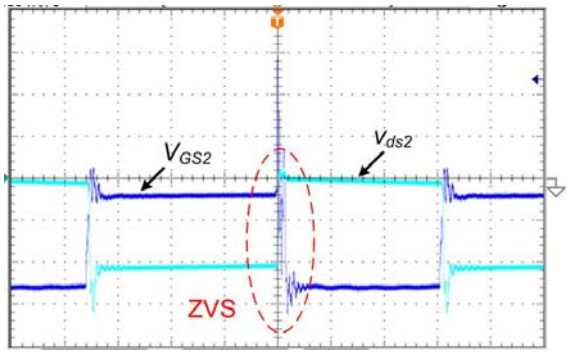

Figure 10. Measured voltage waveforms of the auxiliary switch S_2 at full load operation (v_{ds2}: 20 V/div; v_{GS2}: 5 V/div; time: 1 μs/div).

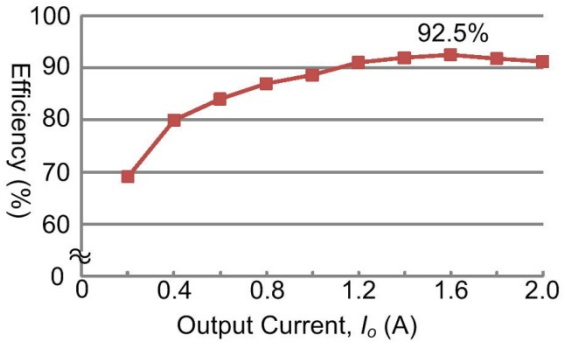

Figure 11. Measured efficiency curve of the proposed color LED driver.

Figure 12 shows the measured waveforms of output voltage V_o and output current I_o while the LED module outputs "white" light. It can be seen that red, green, and blue LED arrays are driving in sequential and with the frequency of 30 Hz. The output voltage V_o is around 10.4 V for driving red LEDs, and V_o is regulated to around 11.4 V for driving green and blue LEDs. The duty cycle of each LED is almost 100% so that all of them provide the highest luminance to have "white" light output. In figure 13, the duty cycle of green LEDs is changed to be 50% to reduce the luminance. Since the luminance of red and blue LEDs remain 100%, the color of the light provided by LED modules is "purple". These experimental results verified that a large chromaticity variation can be achieved by low-frequency PWM control. By the way, the photo of the illustrative prototype is shown in figure 14.

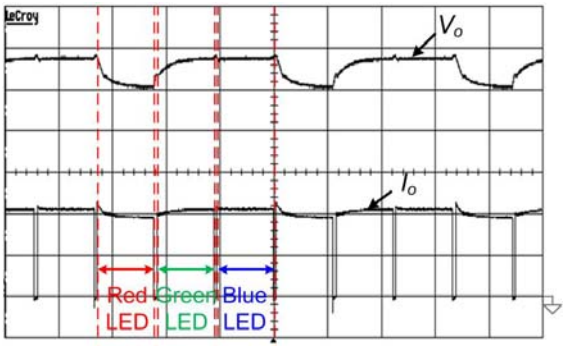

Figure 12. Measured waveforms of output voltage V_o and output current I_o while the LED module outputs "white" light (V_o: 2 V/div; I_o: 500 mA/div; time: 10 ms/div).

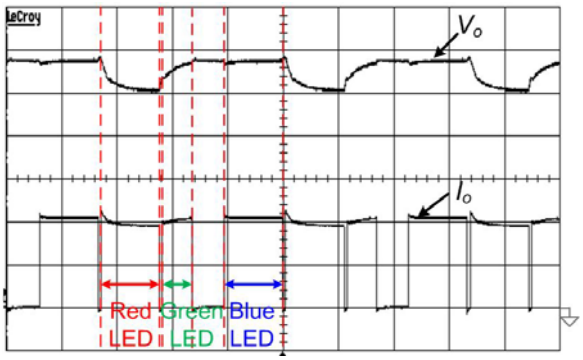

Figure 13. Measured waveforms of output voltage V_o and output current I_o while the LED module outputs "purple" light (V_o: 2 V/div; I_o: 500 mA/div; time: 10 ms/div).

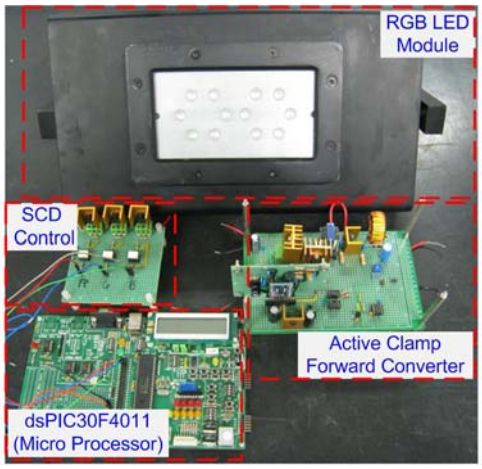

Figure 14. Illustrative prototype of the proposed color LED driver.

5. Conclusion

An active clamp forward converter with the SCD control for driving RGB LED arrays has been proposed. ZVS turn-on operations of both the main switch and the auxiliary switch lead to low switching losses and high system conversion efficiency. RGB LED arrays are sequentially driven by the same converter, which can save components and reduce cost significantly. Besides, PWM control is applied to achieve a large chromaticity variation. Experimental results of a 100 W illustrative example have really proved the feasibility and validity of the theoretical predictions.

Acknowledgements

This work was supported by the National Science Council of Taiwan, Republic of China, under grant contract NSC 101-2221-E-214-059.

References

[1] G. Harbers et al., “Performance of high power light emitting diodes in display illumination applications,” J. Disp. Technol., vol. 3, no. 2, pp. 98–109, Jun. 2007.

[2] S. Muthu et al., “Red, green, and blue LEDs for white light illumination,” IEEE J. Sel. Top Quant., vol. 8, no. 2, pp. 333–338, Mar. / Apr. 2002.

[3] W.-C. Cheng, “Power minimization of LED backlight in a color sequential display,” J. Soc. Inf. Display, vol. 36, no. 1, pp. 1384–1387, May 2005.

[4] F. Gatti et al., “Low power control technique for TFT LCD display,” in proceedings of Compilers, Architecture, and Synthesis for Embedded System, 2002, pp. 218–224.

[5] C.-C. Chen et al., “Sequential color LED backlight driving system for LCD panels,” IEEE T. Power Electr., vol. 22, no. 3, pp. 919–925, May 2007.

[6] Y.-K. Lo et al., “Design and implementation of RGB LED drivers for LCD backlight modules,” IEEE T. Ind. Electron., vol. 56, no. 12, pp. 4862–4871, Dec. 2009.

[7] C. M. C. Duarte and I. Barbi, “A family of ZVS-PWM active-clamping DC-to-DC converters: synthesis, analysis, design, and experimentation,” IEEE T. CIRCUITS–I, vol. 44, no. 8, pp. 698–704, Aug. 1997.

[8] A. Acık and I. Cadırci, “Active clamped ZVS forward converter with soft-switched synchronous rectifier for high efficiency, low output voltage applications,” IET Electr. Power App., vol. 150, no. 2, pp. 165–174, Mar. 2003.

[9] Q. M. Li and F. C. Lee, “Design consideration of the active-clamp forward converter with current mode control during large-signal transient,” IEEE T. Power Electr., vol. 18, no. 4, pp. 958–965, Jul. 2003.